Partial discharges in spheroidal voids: Void orientation

McAllister, Iain Wilson

Published in:
I E E E Transactions on Dielectrics and Electrical Insulation

Link to article, DOI:
10.1109/94.625363

Publication date:
1997

Document Version
Publisher's PDF, also known as Version of record

Partial Discharges in Spheroidal Voids

Void Orientation

I. W. McAllister
Department of Electric Power Engineering, Technical University of Denmark, Lyngby, Denmark

ABSTRACT

Partial discharge transients can be described in terms of the charge induced on the detecting electrode. The influence of the void parameters upon the induced charge is examined and discussed for spheroidal voids. It is shown that a quantitative interpretation of the induced charge requires a knowledge not only of the void location, geometry and dimensions, void gas pressure and composition, but also of the void orientation with reference to the applied field.

1. INTRODUCTION

OVER a period of several years, Pedersen and his colleagues have developed a theory of PD (partial discharge) transients [1–4]. The theory has been used to assess the influence of different void parameters on the charge induced upon a detecting electrode as a result of discharge activity in a bulk void [1]. The present study extends the work reported in [1], by examining the influence of void orientation relative to the direction of the applied field.

A PD in a gaseous void within a bulk dielectric occurs in a closed volume, resulting in a deposition of charge on the void wall. In this confined space, the net charge produced by the discharge will be zero. With respect to the measuring electrode, such a zero net charge configuration may be characterized in terms of its dipole moment [2]. A dipole can induce a net charge on an electrode. Thus the electrical transients associated with PD can be related to changes in the dipole moment of such a wall-charged void.

The Poissonian induced charge q arising from a void dipole of moment $\vec{\mu}$ is

$$q = -\vec{\mu} \cdot \vec{\nabla}\lambda \tag{1}$$

where λ represents the proportionality factor between the void surface charge and the charge induced on the detecting electrode. The function λ is a solution of the general Laplace equation, see [2, 4].

If however the dimensions of the void are so small that $\vec{\nabla}\lambda$ may be assumed constant within the void then we can introduce a related function λ_0, which is derived in the absence of the void. Because λ is a solution of Laplace's equation, then by mathematical analogy with electrostatic fields the relation between the λ and λ_0 functions is given by

$$\vec{\nabla}\lambda = h\vec{\nabla}\lambda_0 \tag{2}$$

For the voids under consideration, the parameter h is a scalar which depends on the void geometry and the relative permittivity of the bulk dielectric. Following the introduction of λ_0, the induced charge on the detecting electrode may be expressed as

$$q = -h\vec{\mu} \cdot \vec{\nabla}\lambda_0 \tag{3}$$

When $\vec{\mu}$ is considered to be associated with the final value of the wall charge density, then q represents the final value of the charge induced on the detecting electrode.

2. INDUCED CHARGE FROM WALL-CHARGED ELLIPSOIDAL VOID

To evaluate the dipole moment of a wall-charged void it was assumed in [1] that the field in the void remained uniform after a PD. On this basis, the Poissonian induced charge q associated with an ellipsoidal void may be expressed as [1]

$$q = -K\Omega\varepsilon(\vec{E}_i - \vec{E}_l) \cdot \vec{\nabla}\lambda_0 \tag{4}$$

where K is a dimensionless parameter which is dependent upon the geometry of the ellipsoid. Ω is the ellipsoid volume and ε is the permittivity of the bulk dielectric. The field strengths E_i and E_l represent the inception field strength for discharge development and the limiting field strength for ionization growth, respectively. That is, a PD can develop when the void field attains a value of E_i and will be quenched when the field is reduced to E_l. This reduction will occur as a consequence of charge separation in the void by the discharge. Due to the applied field, these charges will accumulate at the void wall, and by virtue of their polarities produce a field which opposes the applied field within the void.

It should be noted that h is suppressed in the course of deriving (4). This situation implies that the h factor for the field h_E and the h factor for the λ, h_λ are for this occasion assumed to be identical and thus cancel in (4).

For ellipsoidal voids, it can be shown that K and h are related by [1]

$$h = \frac{K\varepsilon_r}{1 + (K-1)\varepsilon_r} \tag{5}$$

1070–9878/97/$3.00

where ε_r is the relative permittivity of the bulk dielectric. The parameter K is given by

$$K = \frac{2}{abcA} \tag{6}$$

where a, b, c are the semi-axes of the ellipsoid and A represents the integral

$$A = \int_0^\infty \frac{ds}{[(a^2+s)^3(b^2+s)(c^2+s)]^{(1/2)}} \tag{7}$$

in which s is a dummy variable. The parameter A arises from the analysis of the electrostatic field of an ellipsoidal void, in which the external ambient field E_0 is assumed to be parallel to the a axis of the void.

The evaluation of (7) involves the use of elliptic integrals [5], and thus it is preferable to continue the study of the influence of the void parameters upon the induced charge signal with reference to spheroidal voids, *i.e.* we take the a axis to be the axis of rotation and thus $b = c$. In such conditions, A can be expressed in terms of elementary functions.

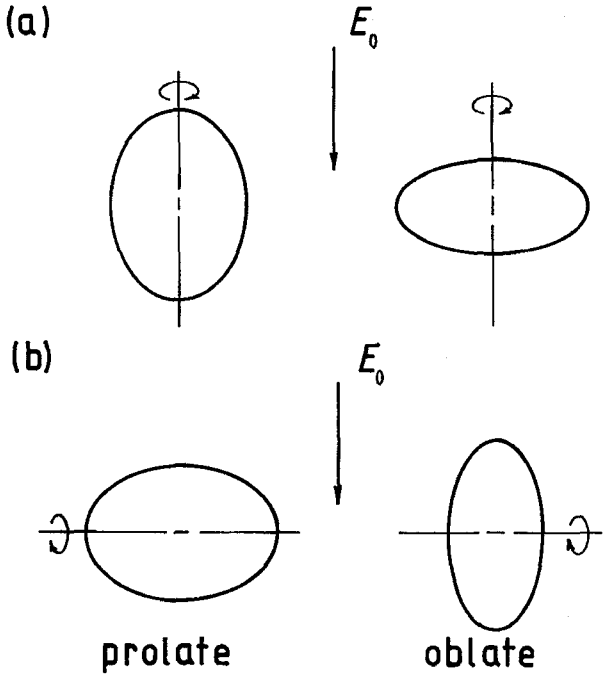

Figure 1. Void orientation with respect to the applied field E_0. (a) E_0 parallel to void axis of rotation (b) E_0 normal to void axis of rotation.

For spheroidal voids, there are two principal orientations of the void with reference to the applied field E_0: E_0 parallel to, or normal to the axis of rotation, see Figure 1. The former condition was discussed in [1]. The latter situation is the subject of the present study. Moreover, as any arbitrary field can be resolved into a component parallel to the void axis and one normal to this axis, it will only be necessary to consider these two conditions.

3. THE K AND h FACTORS FOR SPHEROIDAL VOIDS

Owing to the simplification which occurs with the integral of (7), K can be evaluated readily for spheroidal voids. As (7) relates to E_0 parallel to the a axis, we interchange a and b in this integral expression when considering E_0 normal to the a axis: E_0 is then taken to be parallel to the b axis.

Upon evaluation of the integrals, we obtain for an oblate spheroid $(b/a > 1)$

$$K_p = \frac{u^3}{(u^2+1)(u - \arctan[u])} \tag{8}$$

$$K_n = \frac{2u^3}{(u^2+1)\arctan[u] - u} \tag{9}$$

where the subscripts p and n refer to E_0 being either parallel to, or normal to the axis of rotation, the a axis. The variable u is given by

$$u = \sqrt{(b/a)^2 - 1} \tag{10}$$

Similarly for a prolate spheroid $(b/a < 1)$ we have

$$K_p = \frac{2v^3}{(1-v^2)\left[\ln\left(\frac{1+v}{1-v}\right) - 2v\right]} \tag{11}$$

$$K_n = \frac{4v^3}{(1-v^2)\ln\left(\frac{1-v}{1+v}\right) + 2v} \tag{12}$$

where

$$v = \sqrt{1 - (b/a)^2} \tag{13}$$

The variation of the K parameters is illustrated as a function of the ratio a/b in Figure 2. It is clear that the orientation of E_0 has a major influence upon K. The K_p expressions are identical with the K expressions given in [1].

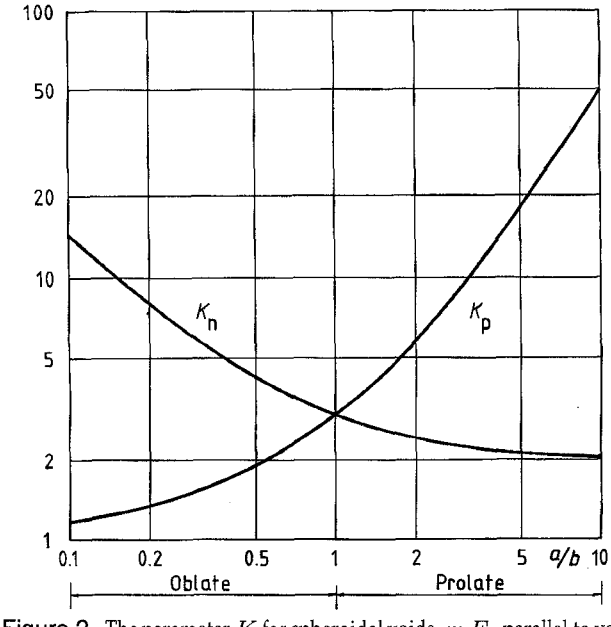

Figure 2. The parameter K for spheroidal voids. p: E_0 parallel to void axis of rotation. n: E_0 normal to void axis of rotation.

With the knowledge of the K values, (5) enables the corresponding h values to be derived. These are shown in Figure 3 for several values of ε_r. The parameter h also represents the proportionality factor between

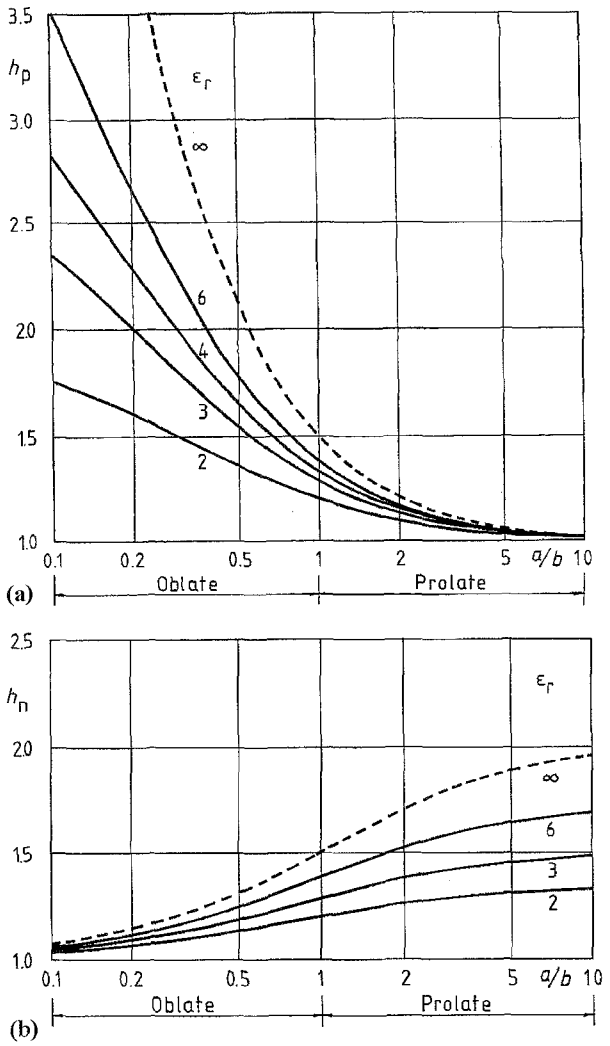

Figure 3. The parameter h for spheroidal voids. (a) E_0 parallel to void axis of rotation: h_p. (b) E_0 normal to void axis of rotation: h_n.

the ambient field E_0 and the uniform field E_1 within the void

$$E_1 = hE_0 \tag{14}$$

Figure 3(a) illustrates the familiar strong field enhancement obtained with oblate spheroidal voids with E_0 parallel to the axis of rotation. However, Figure 3(b) indicates that, with E_0 perpendicular to the axis of rotation, a degree of field enhancement can also arise with prolate spheroidal voids. Consequently it is evident that the question of field enhancement is dependent not only on the void geometry, but also on the void orientation with respect to the ambient field. It should be noted that although the analysis is undertaken with reference to the void axis, it is more appropriate in the subsequent discussions to employ the ambient field direction as reference.

4. SHAPE FACTORS FOR SPHEROIDAL VOIDS

In [1] Crichton *et al.* employed the streamer criterion to evaluate the minimum value of the difference $(E_i - E_l)$ for both strongly attaching and weakly or non-attaching gases: *viz.*, for an attaching gas, we have

Table 1. Shape factors for spheroidal voids.

gas type	void shape	E_0 factor	
		$\parallel$ axis	$\perp$ axis
strongly attaching	k_Ω	$\frac{1}{3}K_p(\frac{a}{b})^{-2/3}$	$\frac{1}{3}K_n(\frac{a}{b})^{1/3}$
	k_a	$\frac{1}{3}K_p(\frac{a}{b})^{-2}$	$\frac{1}{3}K_n(\frac{a}{b})^{-1}$
	k_b	$\frac{1}{3}K_p$	$\frac{1}{3}K_n(\frac{a}{b})$
weakly or non-attaching	k_Ω	$\frac{1}{3}K_p(\frac{a}{b})^{-1/3}$	$\frac{1}{3}K_n(\frac{a}{b})^{1/6}$
	k_a	$\frac{1}{3}K_p(\frac{a}{b})^{-2}$	$\frac{1}{3}K_n(\frac{a}{b})^{-3/2}$
	k_b	$\frac{1}{3}K_p(\frac{a}{b})^{1/2}$	$\frac{1}{3}K_n(\frac{a}{b})$

$$E_i - E_l = \frac{ME_l}{z_0 p} \tag{15}$$

while for a non-attaching gas

$$E_i - E_l = \frac{BE_l}{\sqrt{z_0 p}} \tag{16}$$

where M is the figure of merit for a strongly electronegative gas [6], and B is a characteristic constant for a weakly or non-attaching gas. The length z_0 represents the maximum avalanche path length in the field direction, *i.e.* either $z_0 = 2a$ in the axial direction, or $z_0 = 2b$ in the transverse direction. The parameter p denotes the pressure of the gas within the void.

To indicate the variation of induced charge with void geometry, we select the induced charge associated with a spherical void as a reference level. Introducing a dimensionless shape factor k allows the induced charge to be expressed as [1]

$$q = kq_1 \tag{17}$$

where q_1 is the induced charge for $a/b = 1$, *i.e.* for a spherical void.

For a fixed void location and a constant gas pressure in the void, the influence of void geometry can be illustrated with reference to the different parameters, *viz.* constant void volume: k_Ω, constant a: k_a and constant b: k_b. Taking account of (4), (15), (16) and the volume of a spheroid ($\Omega = 4\pi ab^2/3$), the different shape factors for both attaching and non-attaching gases can be derived. These are listed in Table 1 for the two orientations of the void with respect to the field direction.

With a constant gas pressure, a fixed discharge path length in the field direction implies that the difference $(E_i - E_l)$ will also be constant, irrespective of the void geometry. Thus, owing to the comparative basis of the shape factor, the relevant factor will be independent of the gas type. Hence for E_0 parallel to the axis of rotation, a common k_a expression will be obtained, see Table 1, column 3. Likewise for E_0 normal to the axis of rotation, a common k_b expression is obtained, see Table 1, column 4.

The variation of k_Ω with the axes ratio a/b is shown in Figure 4. An explanation for such non-monotonic k_Ω variations can be found by examining the behavior of the (a/b) functions in the k_Ω expressions. In

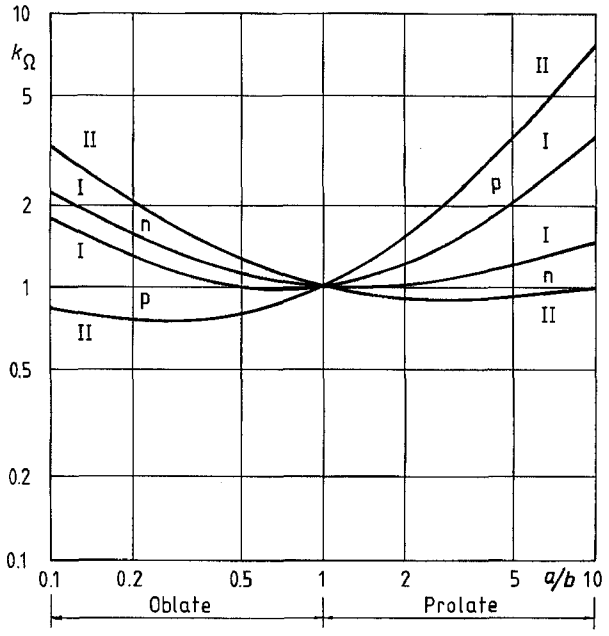

Figure 4. The shape factor k_Ω for spheroidal voids. I: strongly attaching gas, II: weakly or non-attaching gas. p: E_0 parallel to void axis of rotation. n: E_0 normal to void axis of rotation.

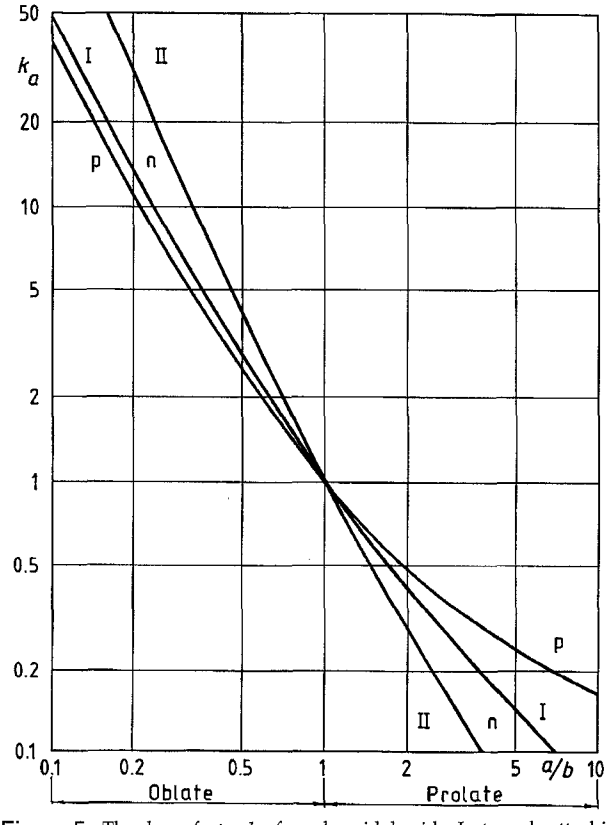

Figure 5. The shape factor k_a for spheroidal voids. I: strongly attaching gas, II: weakly or non-attaching gas p: E_0 parallel to void axis of rotation. n: E_0 normal to void axis of rotation.

each case, the slope of the (a/b) function is the reverse of that for the respective K function. Consequently k_Ω will exhibit a minimum value.

The variations of k_a and k_b with a/b are shown in Figures 5 and 6. In

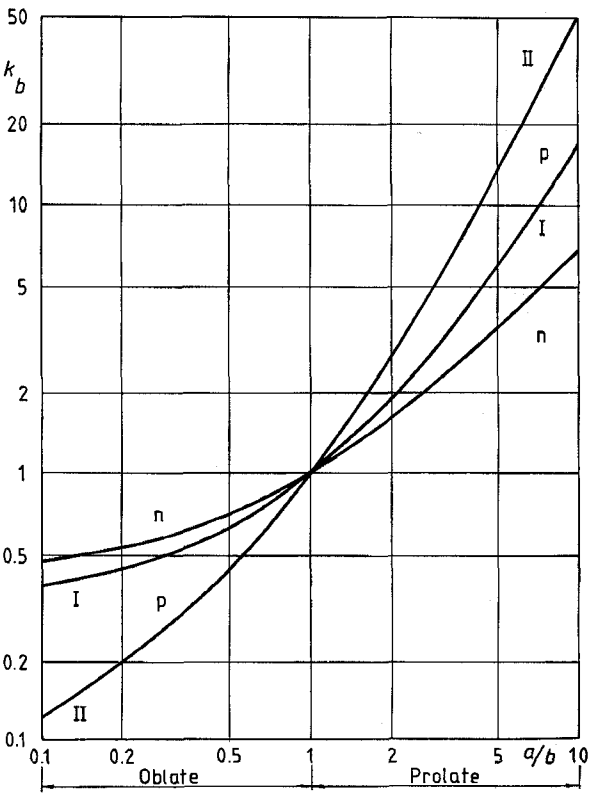

Figure 6. The shape factor k_b for spheroidal voids. I: strongly attaching gas, II: weakly or non-attaching gas p: E_0 parallel to void axis of rotation. n: E_0 normal to void axis of rotation.

contrast to the k_Ω variations, both k_a and k_b vary monotonically with a/b. As discussed above, a common k_a variation, which decreases with increasing a/b, is obtained when E_0 is parallel to the axis of rotation. For $0.1 < a/b < 10$, we have $1 < K_p < 50$, and hence $(a/b)^{-2}$ is the dominant parameter for k_a, (Table 1). For a constant a, the behavior is basically related to the decreasing volume of the spheroidal void as a/b increases. A similar k_a behavior is obtained for E_0 normal to the axis of rotation. On this occasion, the decrease is associated with a decreasing discharge path length, allied with a decreasing K_n. However as is seen from Figure 5, the variation of k_a is similar for each gas type.

The parameter k_b exhibits a common behavior for the two gas types when E_0 is in the b direction, *i.e.* normal to the axis of rotation. For the range $0.1 < a/b < 10$, K_n lies in the range $15 > K_n > 2$, and thus, with reference to k_b in Table 1, the influence of a/b outweighs that of K_n. Consequently k_b increases with a/b. For the same a/b range, but with E_0 parallel to the axis of rotation, we have $1 < K_p < 50$ and hence k_b is the product of two increasing functions. Thus the latter E_0 condition will lead to a more rapidly increasing function of a/b than the former. Essentially the same behavior is exhibited by both gas types.

Introduction of the shape factors allows the specific influence of different parameters to be studied with reference to the induced charge q_1. For a spherical void we have

$$q_1 = -3\Omega\varepsilon(\vec{E}_i - \vec{E}_l) \cdot \vec{\nabla}\lambda_0 \qquad (18)$$

For a void in a fixed location, *i.e.* the system parameter $\vec{\nabla}\lambda_0$ is constant, substitution of (15) or (16) for $(E_i - E_l)$ in (18) indicates that, for

a strongly electronegative gas,

$$q_1 \propto \varepsilon d^2 \tag{19}$$

whereas

$$q_1 \propto \varepsilon\sqrt{pd^5} \tag{20}$$

for a weakly or non-attaching gas. d represents the diameter of the spherical void. For the former case, q_1 is independent of gas pressure. The strong influence of the void dimension is evident in each case.

5. APPLICATION OF THEORY TO A VOID IN A COAXIAL DISC SPACER

To illustrate the foregoing theory, consider a spheroidal void in a simple disc spacer, for which $\varepsilon_r = 4$. The spacer supports the inner conductor of a coaxial electrode system. The radius r_1 of this conductor is 70 mm, while the inner radius r_2 of the outer conductor is 190 mm. The void, the center of which is located at $r = 100$ mm from the axis of the system, has a (constant) volume of 1 mm^3 and is filled with either air or SF_6 at a pressure of 0.1 MPa.

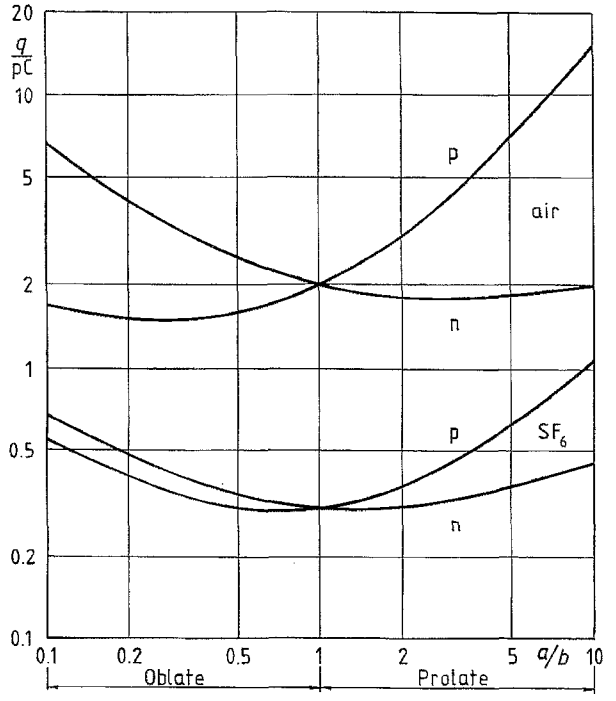

Figure 7. Poissonian induced charge q for spheroidal voids in a coaxial disc spacer. See text for conditions. p: E_0 parallel to void axis of rotation. n: E_0 normal to void axis of rotation.

If the complete inner electrode is employed to detect the PD transient, then $\vec{E}_0$ and $\vec{\nabla}\lambda_0$ are parallel. Thus we have for this simple geometry

$$\vec{\nabla}\lambda_0 = -\frac{\vec{e}_r}{r\ln(r_2/r_1)} \tag{21}$$

where $\vec{e}_r$ is a unit vector perpendicular to the axis of the coaxial system and directed away from the inner electrode. Hence by combining (4), (15), (16) and (21), the induced charge q_1 for a spherical void can be evaluated. Thereafter by employing the different shape factors, the variation of the induced charge for spheroidal voids is obtained directly from (17). Such a variation is shown in Figure 7 as a function of a/b for the case of a constant void volume, *i.e.* with respect to k_Ω.

Although Figure 7 shows the same non-monotonic behavior as found in Figure 4, the former now illustrates the significant influence of the void gas upon the induced charge. The electrically stronger SF_6 provides a much smaller induced charge than the electrically weaker air. This situation arises quite simply because the difference $(E_i - E_l)$ is in general much less for SF_6 than for air.

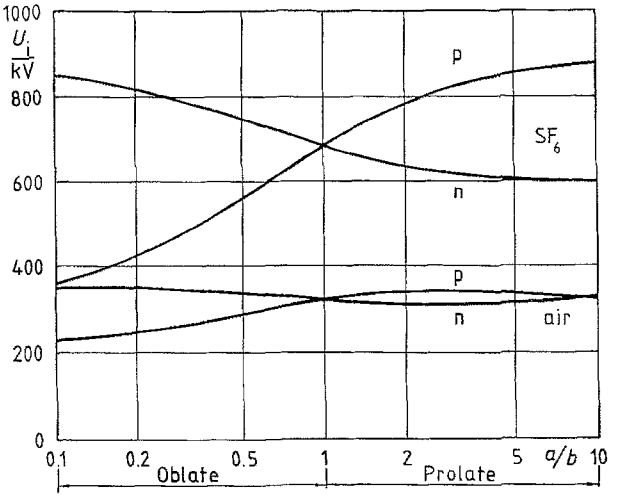

Figure 8. Discharge inception voltages U_i for the voids referred to in Figure 7. p: E_0 parallel to void axis of rotation. n: E_0 normal to void axis of rotation.

On the basis of (15), (16) and the field associated with the coaxial geometry, the corresponding discharge inception voltage U_i can be derived; *viz.*

$$U_i = \frac{E_i}{h} r \ln\left(\frac{r_2}{r_1}\right) \tag{22}$$

Using the data given in [1], the values of U_i for air and SF_6 were evaluated and these are shown in Figure 8. E_i is controlled essentially by E_l. Thus as $E_l(SF_6) \gg E_l(\text{air})$, the inception voltages for SF_6 will be higher than those for air, all other parameters being equal, see Figure 8. As indicated previously, the influence of void orientation is again evident.

With a constant gas pressure, the E_i variations with a/b will not change. Hence for a fixed void location, U_i variations will be inversely proportional to h. From Figure 3, it is evident that depending on the orientation of the void, ε_r has either a significant or a negligible effect on h. Such behavior will also be reflected in the variation of U_i with ε_r.

The shape factors k_a and k_b can be used in an identical manner to that shown above for k_Ω.

6. CONCLUSIONS

PREVIOUSLY, it had been shown in [1] that a unique interpretation of the induced charge produced by a PD in a single void would require a knowledge of void location, geometry and dimensions, void gas pressure and composition: *i.e.* for a given void, there is no unambiguous

relation between the size of the void (volume) and the discharge magnitude (induced charge). It is now demonstrated that the magnitude of the induced charge is strongly dependent on the orientation of the void with respect to the applied field direction. Lack of this knowledge places a further restriction on the achievement of a unique interpretation of the induced charge.

A knowledge of all the above parameters is a prerequisite for a correct quantitative assessment of a PD transient. It is highly improbable that such a combined knowledge will be available for measurements made on actual equipment. Consequently, one can conclude that PD measurements on practical equipment can only be handled meaningfully in terms of pattern recognition. However the present study suggests that, in practice, pattern comparisons would best be restricted to similar equipment produced by a single manufacturer. In such cases the many parameters controlling the induced charge signal remain essentially identical, and thus meaningful comparisons could be effected.

REFERENCES

[1] G. C. Crichton, P. W. Karlsson and A. Pedersen, "Partial Discharges in Ellipsoidal and Spheroidal Voids", IEEE Trans. Elect. Insul., Vol. 24, pp. 335–342, 1989.

[2] A. Pedersen, G. C. Crichton and I. W. McAllister, "The Theory and Measurement of Partial Discharge Transients", IEEE Trans. Elect. Insul., Vol. 26, pp. 487–497, 1991.

[3] A. Pedersen, G. C. Crichton and I. W. McAllister, "Partial Discharge Detection: Theoretical and Practical Aspects", IEE Proc. - Science, Measurement and Technology, Vol. 142, pp. 29–36, 1995.

[4] A. Pedersen, G. C. Crichton and I. W. McAllister, "The Functional Relation between Partial Discharges and Induced Charge", IEEE Trans. Dielect. and Elect. Insul., Vol. 2, pp. 535–543, 1995.

[5] J. A. Stratton, *Electromagnetic Theory*, McGraw-Hill, New York, pp. 207–217, 1941.

[6] A. Pedersen, I. W. McAllister, G. C. Crichton and S. Vibholm, "Formulation of the Streamer Breakdown Criterion and its Application to Strongly Electronegative Gases and Gas Mixtures", Archiv für Elektrotechnik, Vol. 67, pp. 395–402, 1984.

A preliminary version of this paper was published at the 9th Int. Symposium on High Voltage Engineering, Graz, Austria, 1995

Manuscript was received on 8 March 1997, in revised form 29 July 1997.